



Key roles of amylopectin synthesis and degradation enzymes in the establishment and reactivation of chronic toxoplasmosis

Pu Chen¹, Congcong Lyu¹, Yidan Wang¹, Ming Pan¹, Xingyu Lin¹ and Bang Shen^{1,2,3,4,5*}

Abstract

Toxoplasma gondii (*T. gondii*) is an obligate intracellular parasite with a wide range of hosts, including humans and many warm-blooded animals. The parasite exists in two interconvertible forms, namely tachyzoites and bradyzoites in intermediate hosts that are responsible for acute and chronic infections respectively. Mature bradyzoites accumulate large amounts of amylopectin granules but their roles have not been fully characterized. In this study, the predicted key enzymes involved in amylopectin synthesis (UDP-sugar pyrophosphorylase, USP) and degradation (alpha-glucan water dikinase, GWD) of ME49 strain were individually knocked out, and then bradyzoite-related phenotyping experiments in vitro and in vivo were performed to dissect their roles during parasite growth and development. Deletion of the *usp* or *gwd* gene in the type II strain ME49 reduced the replication rates of tachyzoites in vitro and parasite virulence in vivo, suggesting that amylopectin metabolism is important for optimal tachyzoite growth. Interestingly, the Δusp mutant grew slightly faster than the parental strain under stress conditions that induced bradyzoite transition, which was likely due to the decreased efficiency of bradyzoite formation of the Δusp mutant. Although the Δgwd mutant could convert to bradyzoite robustly in vitro, it was significantly impaired in establishing chronic infection in vivo. Both the Δusp and Δgwd mutants showed a dramatic reduction in the reactivation of chronic infection in an in vitro model. Together, these results suggest that USP and GWD, which are involved in amylopectin synthesis and degradation have important roles in tachyzoite growth, as well as in the formation and reactivation of bradyzoites in *T. gondii*.

Keywords *Toxoplasma gondii*, Amylopectin metabolism, Bradyzoites, Reactivation, Chronic infection

*Correspondence:

Bang Shen

shenbang@mail.hzau.edu.cn

¹ State Key Laboratory of Agricultural Microbiology, College of Veterinary Medicine, Huazhong Agricultural University, Wuhan, Hubei Province, PR China

² Key Laboratory of Preventive Veterinary Medicine in Hubei Province, Wuhan, Hubei Province, PR China

³ Hubei Hongshan Laboratory, Wuhan, Hubei Province, PR China

⁴ Shenzhen Institute of Nutrition and Health, Huazhong Agricultural University, Shenzhen, Guangdong Province, PR China

⁵ Shenzhen Branch, Guangdong Laboratory for Lingnan Modern Agriculture, Genome Analysis Laboratory of the Ministry of Agriculture, Agricultural Genomics Institute at Shenzhen, Chinese Academy of Agricultural Sciences, Shenzhen, Guangdong Province, PR China

Introduction

Toxoplasma gondii can infect almost all warm-blooded animals, making toxoplasmosis a serious public health problem worldwide (Kim and Weiss 2004). Obligate intracellular pathogens have coevolved with their host, leading to clever strategies to access nutrients, to evade the host's immune response, and to establish a safe niche for intracellular replication (Krishnan and Soldati-Favre 2021). *T. gondii* has a complex life cycle, that plays key roles in the transmission of this parasite. Within intermediate hosts, *T. gondii* can interconvert between fast replicating tachyzoites and slowly growing bradyzoites, which are responsible for acute and chronic stages of infection



© The Author(s) 2023. **Open Access** This article is licensed under a Creative Commons Attribution 4.0 International License, which permits use, sharing, adaptation, distribution and reproduction in any medium or format, as long as you give appropriate credit to the original author(s) and the source, provide a link to the Creative Commons licence, and indicate if changes were made. The images or other third party material in this article are included in the article's Creative Commons licence, unless indicated otherwise in a credit line to the material. If material is not included in the article's Creative Commons licence and your intended use is not permitted by statutory regulation or exceeds the permitted use, you will need to obtain permission directly from the copyright holder. To view a copy of this licence, visit <http://creativecommons.org/licenses/by/4.0/>. The Creative Commons Public Domain Dedication waiver (<http://creativecommons.org/publicdomain/zero/1.0/>) applies to the data made available in this article, unless otherwise stated in a credit line to the data.

respectively. Such interconversion occurs as a result of the parasite's response to the changes in environmental cues such as the host's immune functions (Dubey 2002; Hunter and Sibley 2012; Lourido 2019).

Due to the limitations of current drugs for the treatment of toxoplasmosis, there is an urgent need for the discovery of new therapeutic options (Xu et al. 2023). The transition of tachyzoites into bradyzoites is thought to be a stress response that associates with the changes of gene expression, metabolism, and morphology (Denton et al. 1996; Lyons et al. 2002; Tu et al. 2018), some of which may be potential targets for the development of drugs and vaccines (Wang et al. 2023). Unlike tachyzoites, bradyzoites accumulate large amounts of amylopectin and exhibit slower growth rates (Ferguson and Hutchison 1987), indicating that bradyzoites have fundamental differences in metabolism compared to tachyzoites. Amylopectin has been shown to play roles in the biology of many Apicomplexa parasites. For example, a reduction in amylopectin levels in *Eimeria tenella* oocysts is associated with decreased oocyst viability and infectivity (Ryley et al. 1969). Deletion of *T. gondii*'s amylopectin-degradation enzyme α -amylase leads to a significant decrease in virulence (Yang et al. 2020), while deletion of the amylopectin-synthesizing enzyme starch synthetase impairs activation of bradyzoites to tachyzoites (Lyu et al. 2021). Nonetheless, the overall functions of amylopectin and its metabolic enzymes in *T. gondii* have not been fully appreciated.

Previous studies have identified the enzymes involved in the synthesis and degradation of amylopectin in *T.*

gondii (Lyu et al. 2021). However, these studies did not fully elucidate the role of amylopectin at different stages of the life cycle of *T. gondii*. In this study, we focused on the first committed step in amylopectin synthesis (the formation of UDP-glucose catalyzed by USP) and the key enzyme GWD involved in amylopectin degradation, to assess the roles of amylopectin metabolic enzymes in *T. gondii*.

Results

Sequence analyses of *TgUSP* and *TgGWD*

To study the role of amylopectin homeostasis in *T. gondii*, we focused on two proteins encoded by TGME49_218200 and TGME49_214260, which are predicted to be key enzymes involved in amylopectin synthesis and degradation (Lyu et al. 2021), respectively. TGME49_218200 is annotated as UDP-sugar pyrophosphorylase (USP), which functions to catalyze the reversible transfer of the uridyl group from UTP to sugar-1-phosphate (Kleczkowski et al. 2011), producing UDP-sugar for amylopectin synthesis. On the other hand, TGME49_214260 is annotated as an alpha-glucan water dikinase. In starch metabolism, the role of GWD is to phosphorylate the glucosyl residues of amylopectin to initiate amylopectin degradation (Mahlow et al. 2016). The expression of both genes was slightly upregulated at the chronic infection stage compared to the acute infection stage (data from ToxoDB) (Pittman et al. 2014).

The results of a BLAST search and amino acid sequence analysis found that USP has a UDPGP domain, which is similar to other UDP-glucose

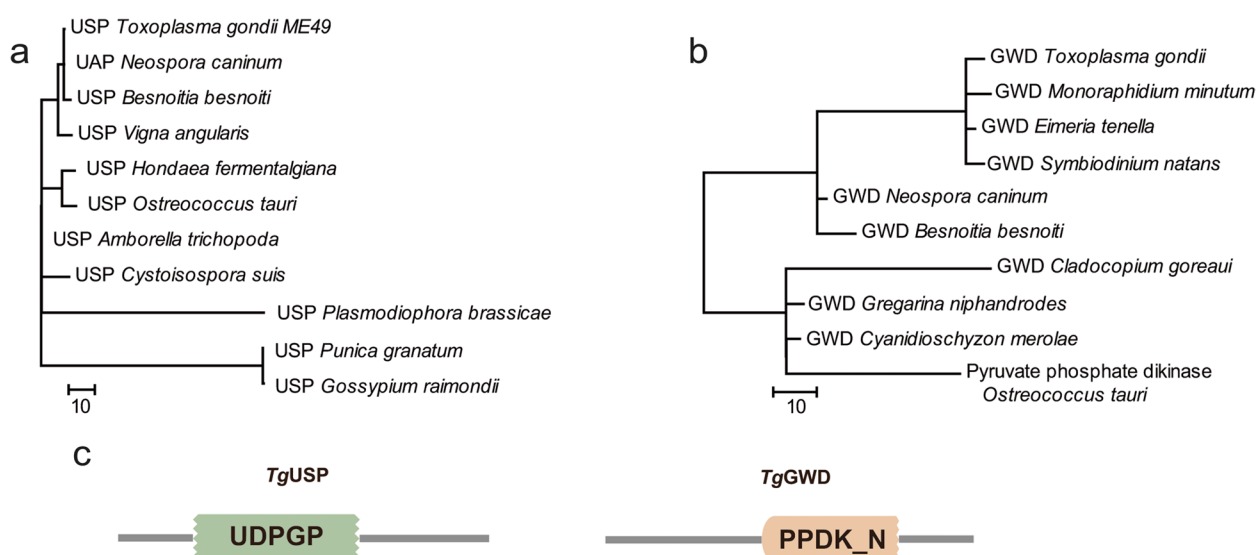


Fig. 1 Sequence analysis of *TgUSP* and *TgGWD*. **a, b** Phylogenetic relationship between *TgUSP* or *TgGWD* and related proteins from other parasites and homologous species. BLAST analysis of protein sequences was performed using the NCBI database, and evolutionary analyses were conducted in MEGA7. **c** Domain structure of *TgUSP* and *TgGWD* predicted by EMBL-EBI using the PFAM database

pyrophosphorylase (UDPGP) family genes (Fig. 1a and c) and suggests that it may be a UDPGP. Homology analysis revealed that *TgUSP* was homologous to certain UDP-N-acetylglucosamine pyrophosphorylases (UAPs). USP was also found in other apicomplexan parasites that accumulate amylopectin, such as *Neospora caninum*, *Besnoitia besnoti*, and *Cystoisospora suis*, while they were not found in apicomplexan species that do not accumulate amylopectin. Additionally, USP was also found in angiosperms and plants with strong environmental resistance, such as *Amborella trichopoda*, *Plasmodiophora brassicae*, and *Gossypium raimondii*. GWD contains a PPDK domain that is commonly found in amylopectin-associated proteins such as amylopectin-associated proteins R1 or alpha-glucan water dikinases (Fig. 1b and c). Phylogenetic analysis revealed that *TgGWD* was closely related to GWDs from algae, such as *Monoraphidium minutum*. GWD was also only found in apicomplexan parasites that accumulate amylopectin, such as *Eimeria tenella*, *Neospora caninum*, and *Besnoitia besnoti*.

Deletion of *usp* and *gwd* led to altered amylopectin accumulation

To investigate the physiological functions of USP and GWD in *T. gondii*, we used the CRISPR/Cas9-mediated homologous gene replacement strategy to directly delete the *usp* and *gwd* genes in the type II strain ME49 (Fig. 2a). CRISPR plasmids targeting the *usp* and *gwd* genes, along with their corresponding homologous templates (5H-DHFR^{*}-3H), were cotransfected into ME49, and positive clones were obtained after pyrimethamine screening. Diagnostic PCRs were used to confirm the direct knockout of the *usp* or *gwd* gene (Fig. 2b) in clonal mutants. The diagnostic PCRs for the Δusp mutant showed the presence of an ~1.5 kb PCR1 product and an ~1.5 kb PCR2 product, indicating that the DHFR^{*} drug screening marker was integrated at the *usp* locus. The absence of an ~0.8 kb PCR3 product amplified from the *usp* gene further confirmed the knockout of this gene (Fig. 2b). Similarly, diagnostic PCR for the Δgwd mutant confirmed the gene-level knockout of *gwd* (Fig. 2b). In addition, quantitative RT-PCR analysis using total RNA extracted from Δusp and Δgwd strains suggested that

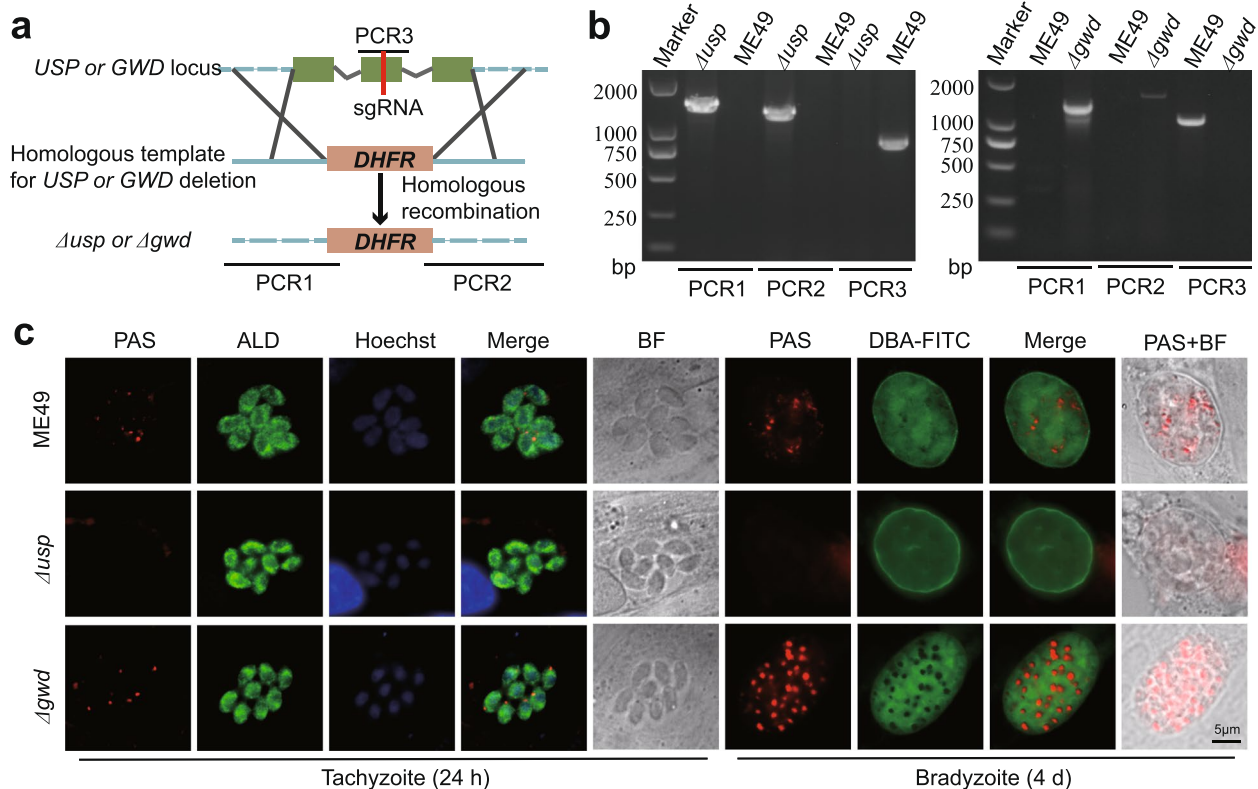


Fig. 2 The *TgUSP* and *TgGWD* deletion strains displayed altered amylopectin metabolism. **a** Schematic illustration of the construction of the Δusp or Δgwd mutant by CRISPR/CAS9-mediated homologous gene replacement in ME49. **b** Diagnostic PCRs on Δusp or Δgwd clones. **c** PAS staining to detect the amylopectin contents in parasites, which were cultured under normal tachyzoite growth conditions for 24 h or bradyzoite-inducing conditions (pH 8.2 and ambient CO₂) for 4 days. The samples were stained with anti-*TgALD*, DBA-FITC, PAS, and Hoechst, to visualize parasites, the cyst wall, amylopectin granules and nuclei, respectively

the expression of USP or GWD in the corresponding mutants was dramatically reduced (Fig. S1), further verifying the deletion of the target genes.

To determine the role of *USP* or *GWD* in amylopectin metabolism in *T. gondii*, periodic acid-Schiff (PAS) staining was used to measure the content of amylopectin in wild-type and mutant parasites. Under normal culture conditions, ME49 tachyzoites showed weak PAS staining, indicating a relatively low level of amylopectin. In contrast, no red PAS signal was detected in the Δusp mutant, suggesting a lack of amylopectin. In the Δgwd mutant, weak PAS staining similar to ME49 tachyzoites was observed, which means that the accumulation of amylopectin had not changed significantly in tachyzoites upon GWD deletion. Under bradyzoite-inducing conditions for 4 days, most vacuoles of the ME49 strain were stained positive for DBA-FITC, showing that they were converted to bradyzoites (Fig. 2c). The PAS staining signal in ME49 bradyzoites was significantly higher than that in tachyzoites, indicating higher accumulation of amylopectin in bradyzoites. Similarly, the Δgwd mutant showed much stronger PAS staining than ME49 bradyzoites, suggesting further increased amylopectin accumulation. In

contrast, no PAS signal was detected in the Δusp mutant even under bradyzoite growth conditions. These results further confirmed that USP was required for the synthesis of amylopectin, while GWD was involved in its degradation.

Both USP and GWD are required for the optimal growth of tachyzoites

Although the direct knockout of *usp* or *gwd* genes suggests that they were not essential for parasite survival, we still attempted to investigate the effect of these two genes on *T. gondii* growth. Therefore, plaque assays were used to evaluate the overall growth of the two mutants. After growth in 6-well plates for 14 d, the number of plaques produced by both mutants was almost the same as that of the wild-type strain ME49 (Fig. 3a and c). However, when the size of the plaques was compared, significant differences were found between the mutant strains and the ME49 strain (Fig. 3b and d), with the plaques of the mutant strains being significantly smaller than those of the ME49 strain. These results indicated that although *TgUSP* and *TgGWD* are not essential, they have a role in the optimal growth of tachyzoites in vitro.

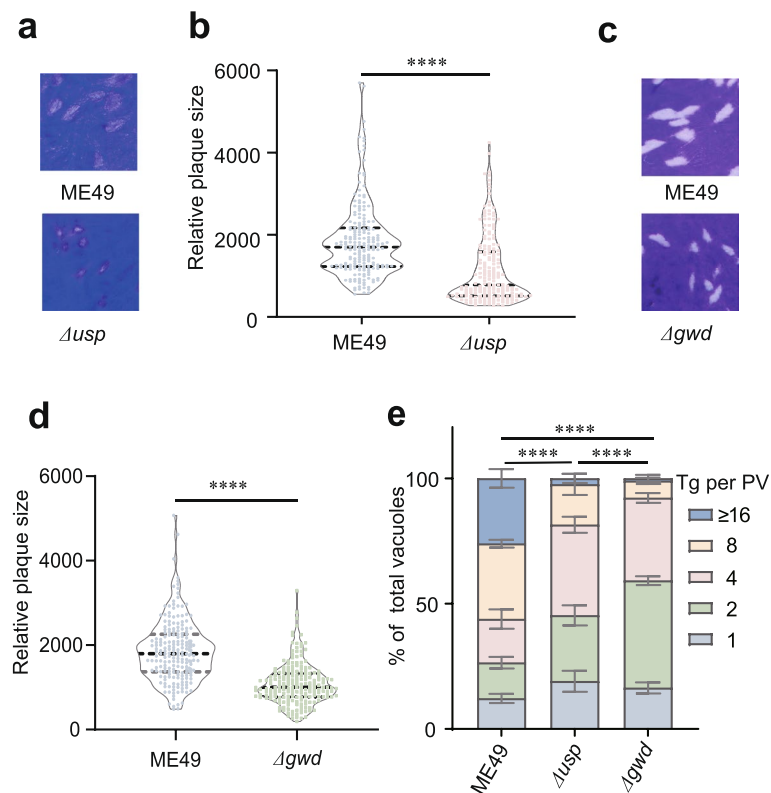


Fig. 3 Reduced growth of the Δusp or Δgwd mutant in vitro. **a-c** Plaque assay of ME49 and the Δusp or Δgwd mutant parasites in vitro. **b-d** Relative size of the plaques formed by ME49 versus Δusp or Δgwd strains cultured in HFFs for 14 days. **** $p < 0.0001$, Student's *t*-test. **e** Intracellular replication rates of parasites under normal conditions for 24 h, as determined by the fraction of vacuoles containing 1, 2, 4, 8 and 16 or more parasites. Means \pm S.D.s of four independent experiments, **** $p < 0.0001$, two-way ANOVA

To further explore the effect of the *usp* and *gwd* genes on tachyzoite growth, we evaluated their intracellular replication rates under normal conditions. Parasites were allowed to replicate for 24 h after entering human foreskin fibroblast cells (HFFs). The results showed that in the ME49 strain, more than 50% of parasitophorous vacuoles (PVs) contained eight or more tachyzoites, while in the Δusp and Δgwd mutant strains, more than 80% of PVs contained four or fewer tachyzoites (Fig. 3e). These results indicated that USP and GWD had important roles in parasite replication at the tachyzoite stage.

Inactivation of USP resulted in reduced bradyzoite transition in vitro

The effects of the *usp* and *gwd* genes on the growth of bradyzoites under bradyzoite-inducing conditions were also studied. Parasites were induced for four days and then allowed to replicate for another 36 h after reinventing new HFFs. The results suggested that the number of PVs containing eight or more parasites in the Δusp mutant strain was greater than 50%, which was significantly higher than that of the wild-type ME49 strain, indicating a significant increase in the replication rate of the Δusp mutant under bradyzoite-inducing conditions. On the other hand, the number of PVs containing four or fewer parasites in the Δgwd mutant strain was slightly higher than that in the ME49 strain (Fig. 4a), which indicates reduced replication of the Δgwd mutant.

Deletion of *usp* or *gwd* genes altered parasite growth under stress conditions, suggesting that they may have a role in bradyzoites. To verify this possibility, the impact of these two genes on the efficiency of bradyzoite formation

was assessed. Parasites induced for 4 days were stained with DBA-FITC, which labeled the wall of *Toxoplasma* cysts to estimate the rates of bradyzoite transition. Under this treatment, 90% of the ME49 vacuoles became DBA positive, suggesting robust bradyzoite formation (Fig. 4b). In contrast, the bradyzoite conversion rate of the Δusp mutant was only approximately 15% under the same conditions. On the other hand, the bradyzoite conversion rate of the Δgwd mutant strain was slightly higher than that of ME49, approaching 100% (Fig. 4b). These results suggest that USP and GWD deletions had opposite impacts on bradyzoite conversion.

Deletion of *usp* or *gwd* causes reduced virulence and decreased cyst formation in vivo

To check the importance of USP and GWD during parasite infection in vivo, the parasites were used to infect ICR mice through intraperitoneal injection to monitor virulence. Mice infected with the ME49 strain began to show irreversible signs of death after 12 d, and the mortality rate reached 80% (Fig. 5a). In contrast, the mortality rates of mice infected with the Δusp mutant and Δgwd mutant were reduced to 60% and 50% respectively (Fig. 5a), suggesting that both USP and GWD contributed to the parasite's virulence.

To explore the impact of USP and GWD on chronic infection in vivo, we counted and measured the size of *Toxoplasma* cysts in the brains of mice that survived 30 days after infection. The results showed that the number of cysts produced by both mutant strains was significantly lower than that formed by the ME49 strain (Fig. 5b). In addition, the average diameter of cysts derived from the mutant strains was also larger than

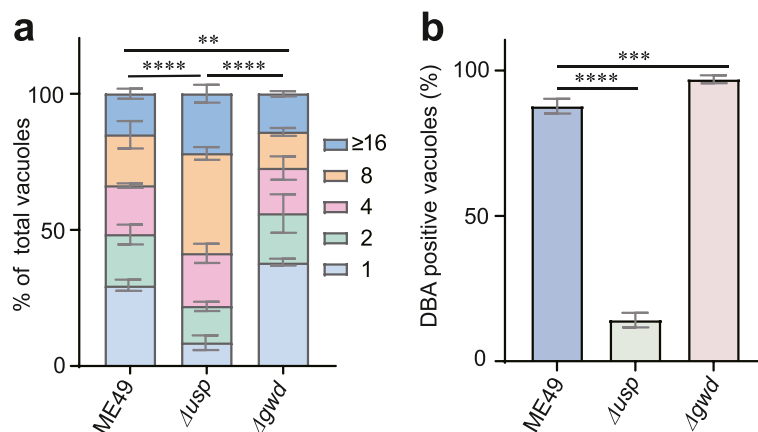


Fig. 4 Deletion of *usp* or *gwd* results in defective growth and formation of bradyzoites. **a** Intracellular replication rates of parasites under bradyzoite-inducing conditions for 36 h, as determined by the fraction of vacuoles containing 1, 2, 4, 8 and 16 or more parasites. Means \pm S.D.s of four independent experiments, **** p < 0.0001, ** p = 0.0074, two-way ANOVA. **b** Bradyzoite conversion assay. Parasites were cultured under bradyzoite-inducing conditions for 4 days before IFA staining to determine the efficiency of bradyzoite transition. Means \pm S.D.s of four independent experiments, ** p = 0.0074, **** p < 0.0001, Student's *t* test

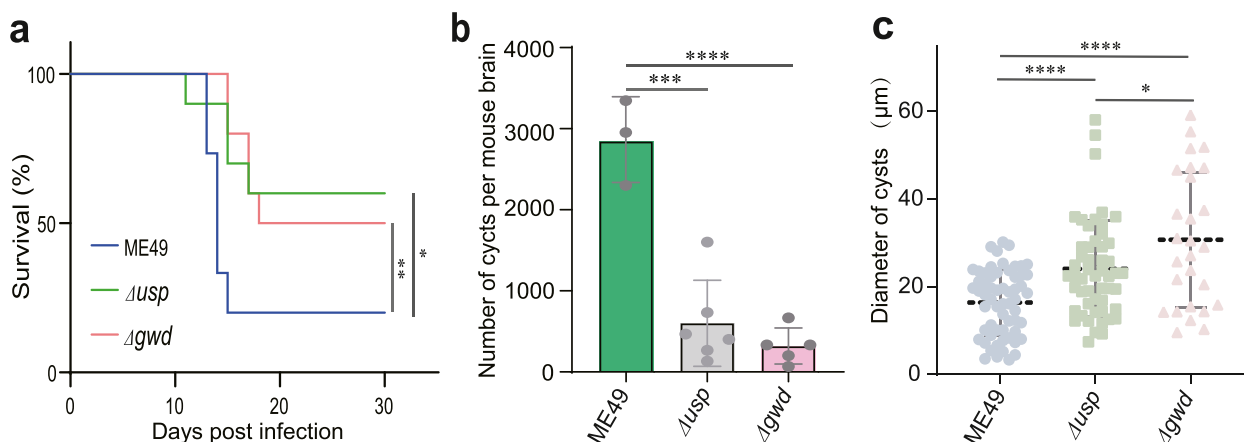


Fig. 5 Deletion of *usp* or *gwd* affects virulence and cyst formation in vivo. **a** Survival curves of ICR mice infected with 100 tachyzoites of the indicated strains ($n = 10$ mice or more), $*p = 0.0218$, $**p = 0.0041$, Gehan–Breslow–Wilcoxon test). **b** *Toxoplasma* cysts in the brains of ICR mice that survived at day 30 in **a**. The brain cysts were collected and stained with DBA-FITC, and then counted. Median with interquartile range, $***p = 0.0006$, $****p < 0.0001$, Student's *t*-test. **c** Relative size (diameter) of brain cysts detected in Fig. 4b, $*p = 0.029$, $****p < 0.0001$, Student's *t* test

that from the ME49 strain (Fig. 5c). The cysts from the mutant were also more heterogeneous in size (Fig. 5c). These observations suggested that both USP and GWD contributed to maintaining normal cyst formation, which was beneficial for the establishment of chronic infection.

Both USP and GWD are needed for the reactivation of bradyzoites to tachyzoites

It has long been believed that amylopectin is an important energy source for the reactivation of bradyzoites to tachyzoites. Using the Δusp and Δgwd mutants, we attempted to verify whether disturbances in amylopectin metabolism affect bradyzoite-to-tachyzoite conversion. Parasites were cultured under bradyzoite-inducing conditions for 12 d. Then they were released from host cells, allowed to invade fresh HFF cells and cultured under normal conditions for an additional 36 h. DBA staining was used to assess the efficiency of bradyzoite-to-tachyzoite conversion. The results showed that bradyzoites of the ME49 wild-type strain were efficiently converted to tachyzoites after shifting the parasites to normal culture conditions, with the proportion of bradyzoites decreasing from approximately 95% to approximately 25% (Fig. 6). In the Δusp mutant, the proportion of bradyzoites decreased from 22 to 14% (Fig. 6) after the same treatment. In contrast, no parasites were detected after 36 h of activation in the Δgwd mutant (Fig. 6), indicating that bradyzoites of the Δgwd mutant were unable to invade HFF cells. These data suggested that USP and GWD played important roles in bradyzoite-tachyzoite reactivation, which implies that amylopectin may provide energy for the conversion of bradyzoites to tachyzoites.

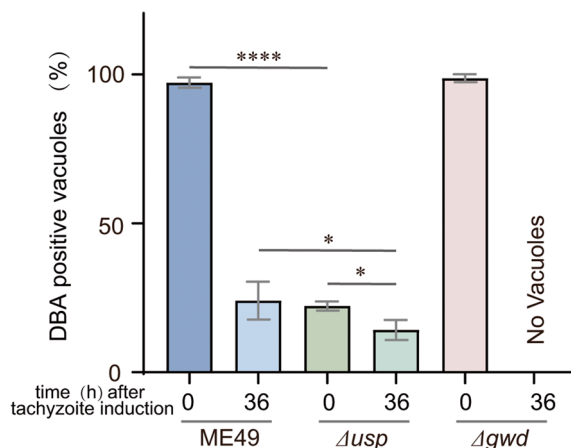


Fig. 6 Reactivation of bradyzoites to tachyzoites in vitro. The parasites were first cultured under bradyzoite-inducing conditions for 12 days to induce bradyzoite formation and then cultured under normal conditions for another 36 h. The samples were stained with DBA-FITC and the decrease in DBA-positive vacuoles indicated that bradyzoites were transformed into tachyzoites. Means \pm S.D.s of four independent experiments, ns represents not significant, $*p = 0.034$, $****p < 0.0001$, Student's *t* test

Discussion

Previous work has shown that tachyzoites and bradyzoites have different energy metabolism characteristics. Bradyzoites accumulate large amounts of amylopectin in their cytoplasm (Guimarães et al. 2003; Guérardel et al. 2005), but their physiological roles have not been firmly established. In this study, two enzymes, USP and GWD involved in amylopectin synthesis and degradation respectively, were deleted in the type II strain ME49 to evaluate their impacts on parasite growth and development. Consistent with previous data, both play roles in the optimal growth of tachyzoites in vitro,

although they are not essential. In addition, USP, which is required for amylopectin synthesis, was critical for the establishment of chronic infection, whereas mutants lacking USP could still establish chronic infection. On the other hand, bradyzoites from the GWD mutants seemed to not be able to invade host cells even after switching to tachyzoite growth conditions. Together, these results suggest that enzymes involved in amylopectin metabolism are important for the optimal growth and activities of *Toxoplasma* tachyzoites and bradyzoites.

The Δusp mutant strain was defective in amylopectin synthesis, while the Δgwd mutant strain resulted in the excess accumulation of amylopectin granules. These results further confirm the function of USP and GWD in the amylopectin metabolism network. Our results indicated that USP and GWD were not essential during the tachyzoite growth phase of *T. gondii*, which means that amylopectin may not be the main source of energy or storage material during the rapid replication stage of *T. gondii*. However, during growth in vivo or the bradyzoite stage, we found that a defect in amylopectin synthesis impaired the formation of bradyzoites, while the inhibition of amylopectin degradation led to excessive conversion of tachyzoites to bradyzoites. This result confirmed that amylopectin was an important energy source for bradyzoite formation (Coppin et al. 2003; Tomavo 2015).

Recent studies have speculated that amylopectin, a complex carbohydrate, may be a key metabolic substance for the development and maintenance of chronic infections in bradyzoites of *T. gondii*, but the specific physiological functions of amylopectin in these stages have not been analyzed (Fayer et al. 1998; Augustine 1980). However, mouse virulence assays showed a significant decrease in virulence for strains with a single knockout of the *USP* and *GWD* genes, although they could both form brain cysts, and we noticed that the number and size of cysts were disrupted. To verify these results, we tested the ability of the mutant strains to reactivate bradyzoites in vitro. The results showed that the bradyzoites of the Δusp mutant strain were responsive to reactivation signals, while those of the Δgwd mutant strain were not, suggesting that the accumulation of amylopectin in bradyzoites may contribute to reactivation of the chronic infection stage of *T. gondii*. On the other hand, bradyzoites of the Δgwd mutant seem to have significantly reduced invasion efficiency. Since invasion requires a large amount of energy, these results suggest that amylopectin degradation may be an important source of energy at the bradyzoite stage, which is consistent with previous hypotheses (Uboldi Alessandro et al. 2015).

Conclusions

Using gene deletion strategies, this study analyzed the functions of two enzymes that are predicted to be involved in amylopectin synthesis and degradation. Inactivation of *USP* led to reduced amylopectin synthesis, whereas deletion of *GWD* caused massive amylopectin accumulation. In addition, deletion of either *USP* or *GWD* reduced the replication rates of tachyzoites in vitro and parasite virulence in vivo. The Δusp mutant displayed reduced efficiency in conversion to bradyzoites, whereas the Δgwd mutant did not seem to have such defects. However, both mutants are significantly impaired in the reactivation of chronic infection in an in vitro model. Together, these results suggest that USP and GWD, which are involved in amylopectin metabolism have important roles in tachyzoite growth, as well as bradyzoite formation and reactivation.

Methods

Parasite strains and growth conditions

All transgenic parasite strains used in this study were derived from the parental strain ME49, and the parasites were cultured in HFFs (purchased from ATCC, USA) under specific culture conditions, as described previously (Ye et al. 2019).

Construction of *usp* and *gwd* deletion mutants

All primers used in this study are listed in Table 1. To generate the CRISPR plasmids targeting *TgUSP* or *TgGWD*, the *UPRT* targeting sequence in pSAG1::CAS9U6::sgUPRT (Addgene #54467) was replaced with gRNAs targeting *TgUSP* or *TgGWD*, using methods described previously (Shen et al. 2014). To obtain the 5'- and 3'-homologous arms of *TgUSP* or *TgGWD* and the DHFR mini gene cassette, PCR was performed on genomic DNA from the ME49 strain and the *pUPRT-DHFR-D* plasmid (Shen et al. 2017), respectively. These fragments were then ligated by homologous recombination into the pUC19 vector using the ClonExpress II One Step Cloning Kit (Vazyme Biotech, China) to obtain a plasmid containing 5H-DHFR-3H, which was used as a template for further PCR amplification (primers U5-USP-Fw and U-3USP-Rv or U5-GWD-Fw and U3-GWD-Rv, Table 1) to obtain an appropriate amount of homologous replacement template for transfection. To obtain gene deletion mutants, 7.5 μ g of the CRISPR plasmid and 1.5 μ g of the homologous replacement template (5H-DHFR-3H) were cotransfected into the parental ME49 strain by electroporation, and pyrimethamine (1 μ M) was used for selection. Single clones were obtained by limited

Table 1 Primers used in this study

Name	Sequence (5' → 3')	Used for
gRNA-USP-Fw	GTCTGTGTACCTCCGTTCTGTTTTAGAGCTAGAAATAGC	To construct the USP-specific CRISPR plasmid
gRNA-GWD-Fw	GCCTGTGCACCAACTTCTTC GTTTTAGAGCTAGAAATAGC	To construct the GWD-specific CRISPR plasmid
gRNA-Rv	AACTTGACATCCCCATTAC	To construct gene-specific CRISPR plasmids
DHRR-Fw	CAGGCTGTAATCCCGTGAG	Amplification of DHFR fragment
DHFR-Rv	GATTCCGTCAGCGGTCTGTC	
U5-USP-Fw	GTGAGGAAACAAGTGCC	Amplification of 5'-homology of USP for 5H-DHFR*-3H construction
U5-USP-Rv	CTCACGGGATTACAGCCTG CGCGTTTCCTTCAGCTT	
U3-USP-Fw	GACAGACCCTGACGGAATC TTTTCGGAGTTCAAGTTGC	Amplification of 3'-homology of USP for 5H-DHFR*-3H construction
U3-USP-Rv	AGGCGAACCTCCACTT	
U5-GWD-Fw	CGACGGCCAGTGAATTCGAG	Amplification of 5'-homology of GWD for 5H-DHFR*-3H construction
U5-GWD-Rv	GATGATTTGTGAGGACGACTCACGGGATTACAGCCTGTC	
U3-GWD-Fw	ACAGACCCTGACGGAATCGGTGCGAGTCAAGAACTCAGG	Amplification of 3'-homology of GWD for 5H-DHFR*-3H construction
U3-GWD-Rv	GCTATGACCATGATTACGCCATCAG	
5'-UpU5USP	GCTCGACATCTTCTCGGAG	PCR1 of <i>Δusp</i>
5'-UpU5GWD	CACGCCACGCTTCTTAATCG	PCR1 of <i>Δgwd</i>
3'-InDHFR	CAAGACGCAGACGCATACAA	PCR1 of <i>Δusp</i> and <i>Δgwd</i>
5'-InDHFR	CGCACGGACGAATCCAGATG	PCR2 of <i>Δusp</i> and <i>Δgwd</i>
3'-DnU3USP	TCAAAGACGACTGCATGC	PCR2 of <i>Δusp</i>
3'-DnU3GWD	AACCTTGCGCTTCAATCC	PCR2 of <i>Δgwd</i>
In-USP-Fw	CCTGGGATCTATTGCTGGA	PCR3 of <i>Δusp</i>
In-USP-Rv	GGCCTGCAGAGAAAAAGAA	
In-GWD-Fw	AACCTTGCGCTTCAATCC	PCR3 of <i>Δgwd</i>
In-GWD-Rv	TCCAGAAAGCCGATGACG	
RT-tubulin-Fw	CACTGGTACACGGGTGAAGGT	β-tubulin-based qRT-PCR
RT-tubulin-Rw	ATTCTCCCTCTTCTCTGCG	
RT-USP-Fw	GTAGTTCTCGCTCCGTCCTG	USP-based qRT-PCR
RT-USP-Rw	CCGTCTTCAAAGGCCATCCT	
RT-GWD-Fw	TCTGAAACGACGTTCCCTCG	GWD-based qRT-PCR
RT-GWD-Rw	TCACGGCGATGATAGTGTCG	

dilution in 96-well plates seeded with HFFs and identified by diagnostic PCRs.

Periodic acid–Schiff staining

For tachyzoite staining, freshly egressed parasites were inoculated onto HFFs seeded on glass coverslips and cultured under standard growth conditions for 24 h. The samples were then subjected to periodic acid-Schiff (PAS) staining following previously described protocols (Xia et al. 2019). For bradyzoite staining, freshly released tachyzoites were inoculated onto HFFs and cultured under standard growth conditions for 2 h, then switched to bradyzoite-inducing conditions (RPMI 1640 medium supplemented with 50 mM HEPES and 1% fetal bovine serum, pH 8.2, ambient CO₂) and cultured for another 4 d before PAS staining. All samples were fixed with 4% paraformaldehyde, permeabilized with 0.1% Triton X-100 (Sigma–Aldrich, USA), and stained with Hoechst 33342 (Beyotime, China) and FITC-conjugated Dolichos

biflorus agglutinin (DBA-FITC) (Vector Laboratories, USA). Subsequent PAS staining was performed according to previously reported procedures (Sugi et al. 2017). In brief, the samples were incubated in 1% periodic acid (Sigma–Aldrich, USA) for 5 min, washed five times with PBS, incubated in Schiff's reagent (Sigma–Aldrich, USA) for 15 min, and washed five times with PBS. After mounting, observation and imaging were performed using an Olympus BX53 microscope (Olympus, Japan) equipped with an Axiocam 503 mono camera (Carl Zeiss, Germany).

Plaque assay

Freshly released tachyzoites were purified by filtration through a 3.0 μm polycarbonate filter membrane, and counted using a hemocytometer under a Nikon Eclipse TS100 phase-contrast microscope (Nikon Instruments, Tokyo, Japan). Subsequently, parasites were seeded at a density of 200 parasites per well in a 6-well plate with

HFFs and allowed to grow without interference for 14 d under standard growth conditions at 37°C and 5% CO₂. Then, samples were fixed with 4% paraformaldehyde and stained with 1% crystal violet. Imaging of the plaques was performed using a scanner, and the number and size of plaques were analyzed and quantified (Shen and Sibley 2014).

Intracellular replication assay

The intracellular replication assay was performed as previously described (Xia et al. 2018). For tachyzoites, freshly released parasites were used to infect monolayers of HFFs on glass coverslips. After 1 h of incubation under standard growth conditions, uninvaded tachyzoites were washed away, and the cells were further incubated for 24 h under standard growth conditions. For bradyzoites, parasites were first cultured for 4 d under bradyzoite-inducing conditions. Then, freshly released parasites were used to infect new monolayers of HFFs on glass coverslips using an injection needle and were further cultured for 36 h under the same bradyzoite-inducing conditions. Extracellular parasites were stained with pig anti-*Toxoplasma* IgG before the sample was permeabilized, and then all parasites were stained with rabbit anti-*TgALD*. After staining with Alexa Fluor 594-conjugated goat anti-rabbit IgG and FITC-conjugated goat anti-pig IgG (Life Technologies, Camarillo, CA, USA), extracellular parasites were simultaneously stained red and green, which were not included in the analysis, while intracellular parasites were only stained red and were counted for analysis (Yang et al. 2022).

Bradyzoite conversion and reactivation assay

The method of inducing bradyzoite differentiation in vitro has been described previously (Yang et al. 2017). Briefly, freshly egressed parasites were used to infect HFFs seeded on glass coverslips. After 1 h of incubation under standard growth conditions, uninvaded tachyzoites were washed away and the cells were cultured for 4 d under bradyzoite-inducing conditions before immunofluorescence analysis was performed. DBA-FITC was used to stain bradyzoites, while rabbit anti-*TgALD* was used to stain all parasites. The differentiation rate of bradyzoites was quantified by counting the number of DBA⁺ / *TgALD*⁺ vacuoles.

For the bradyzoite-to-tachyzoite conversion assay, parasites were first cultured under bradyzoite-inducing conditions for 12 d. Subsequently, freshly excreted parasites were needle released and used to infect new HFFs on glass coverslips. The cells were then cultured under standard tachyzoite growth conditions for another 36 h.

Immunofluorescence analysis was then performed to quantify the conversion rate of bradyzoites to tachyzoites, as described above.

Virulence tests and brain cyst formation in mice

The freshly released tachyzoites were purified by passing through a 3.0 μm polycarbonate filter membrane and then counted using a hemocytometer under a Nikon Eclipse TS100 phase-contrast microscope (Nikon Instruments, Tokyo, Japan). The parasites were then used to intraperitoneally infect 7- to 8-week-old female ICR mice (10 or 15 mice/strain, 100 tachyzoites/mouse). Daily monitoring of the mice for survival was performed for 30 d. The cumulative mortality rate was shown using a Kaplan–Meier survival curve and analyzed using Prism 8 software (GraphPad Software, La Jolla, CA, USA). The infection status of surviving mice was determined by indirect ELISA for the detection of parasite-specific antibodies. Mice with positive serum were euthanized, and their brain tissues were homogenized, followed by staining with DBA-FITC to count the number and measure the size of *Toxoplasma* cysts, as described (Buchholz et al. 2011).

Statistical analysis

Statistical analyses were performed in Prism 8 (GraphPad Software Inc., La Jolla, CA, USA) using Student's *t* test, two-way ANOVA or Gehan–Breslow–Wilcoxon test, as indicated in the figure legends.

Abbreviations

<i>T. gondii</i>	<i>Toxoplasma gondii</i>
USP	UDP-Sugar Pyrophosphorylase
GWD	Alpha-glucan water dikinase
UDPGP	UDP-glucose pyrophosphorylase
UAP	UDP-N-Acetylglucosamine Pyrophosphorylase
PVs	Parasitophorous Vacuoles
HFFs	Human foreskin fibroblasts
DBA	Dolichos biflorus (Horse Gram) agglutinin
FITC	Fluorescein isothiocyanate
PAS	Periodic acid-Schiff

Supplementary Information

The online version contains supplementary material available at <https://doi.org/10.1186/s44149-023-00083-x>.

Additional file 1: Figure S1. RT-PCR examining the transcript levels of *TgUSP* and *TgGWD*.

Acknowledgements

The authors want to thank Ms. Qiong Jiang for help with the cell culture work used in this study.

Authors' contributions

Design of the study and acquisition of funding: Bang Shen; performing the experiments and data analyses: Pu Chen, Congcong Lyu, Yidan Wang, Ming

Pan and Xingyu Lin; drafting of the manuscript: Pu Chen; revision of the article: Bang Shen and Pu Chen.

Funding

This work was supported by the Fundamental Research Funds for the Central Universities in China (Grant no. 2662022DKPY003) and the HZAU-AGIS Cooperation Fund (Grant no. SZYJY2022015).

Availability of data and materials

All data are included in the manuscript and supplementary materials.

Declarations

Ethics approval and consent to participate

Seven- to eight-week-old female ICR mice were purchased from the Hubei Provincial Center for Disease Control and Prevention and housed under standard conditions at the Experimental Animal Center of Huazhong Agricultural University in accordance with the regulations of the Experimental Animal Management Bureau. All animal experiments were approved by the Ethics Committee of Huazhong Agricultural University (permit number: HZAUMO-2019-098).

Consent for publication

All authors confirmed the final version of the manuscript for publication.

Competing interests

The authors have no competing interests to declare. Author Bang Shen was not involved in the journal's review or decisions related to this manuscript.

Received: 18 May 2023 Accepted: 27 May 2023

Published online: 08 June 2023

References

- Augustine, P.C. 1980. Effects of storage time and temperature on amylopectin levels and oocyst production of *Eimeria meleagridis* oocysts. *Parasitology* 81 (Pt 3): 519–524. <https://doi.org/10.1017/S003118200061904>.
- Buchholz, K.R., H.M. Fritz, X. Chen, B. Durbin-Johnson, D.M. Rocke, D.J. Ferguson, et al. 2011. Identification of tissue cyst wall components by transcriptome analysis of in vivo and in vitro *Toxoplasma gondii* bradyzoites. *Eukaryotic Cell* 10 (12): 1637–1647. <https://doi.org/10.1128/ec.05182-11>.
- Coppin, A., F. Dzierszinski, S. Legrand, M. Mortuaire, D. Ferguson, and S. Tomavo. 2003. Developmentally regulated biosynthesis of carbohydrate and storage polysaccharide during differentiation and tissue cyst formation in *Toxoplasma gondii*. *Biochimie* 85 (3–4): 353–361. [https://doi.org/10.1016/S0300-9084\(03\)00076-2](https://doi.org/10.1016/S0300-9084(03)00076-2).
- Denton, H., C.W. Roberts, J. Alexander, K.W. Thong, and G.H. Coombs. 1996. Enzymes of energy metabolism in the bradyzoites and tachyzoites of *Toxoplasma gondii*. *FEMS Microbiology Letters* 137 (1): 103–108. <https://doi.org/10.1111/j.1574-6968.1996.tb08090.x>.
- Dubey, J.P. 2002. Tachyzoite-induced life cycle of *Toxoplasma gondii* in cats. *Journal of Parasitology* 88 (4): 713–717. [https://doi.org/10.1645/0022-3395\(2002\)088\[0713:Tilcot\]2.0.Co;2](https://doi.org/10.1645/0022-3395(2002)088[0713:Tilcot]2.0.Co;2).
- Fayer, R., J.M. Trout, and M.C. Jenkins. 1998. Infectivity of *Cryptosporidium parvum* oocysts stored in water at environmental temperatures. *Journal of Parasitology* 84 (6): 1165–1169. <https://doi.org/10.2307/3284666>.
- Ferguson, D.J., and W.M. Hutchison. 1987. An ultrastructural study of the early development and tissue cyst formation of *Toxoplasma gondii* in the brains of mice. *Parasitology Research* 73 (6): 483–491. <https://doi.org/10.1007/bf00535321>.
- Guérardel, Y., D. Leleu, A. Coppin, L. Liénard, C. Slomianny, G. Strecker, et al. 2005. Amylopectin biogenesis and characterization in the protozoan parasite *Toxoplasma gondii*, the intracellular development of which is restricted in the HepG2 cell line. *Microbes and Infection* 7 (1): 41–48. <https://doi.org/10.1016/j.micinf.2004.09.007>.
- Guimarães, E.V., L. de Carvalho, and H.S. Barbosa. 2003. An alternative technique to reveal polysaccharides in *Toxoplasma gondii* tissue cysts. *Memorias Do Instituto Oswaldo Cruz* 98 (7): 915–917. <https://doi.org/10.1590/S0074-02762003000700010>.
- Hunter, C.A., and L.D. Sibley. 2012. Modulation of innate immunity by *Toxoplasma gondii* virulence effectors. *Nature Reviews Microbiology* 10 (11): 766–778. <https://doi.org/10.1038/nrmicro2858>.
- Kim, K., and L.M. Weiss. 2004. *Toxoplasma gondii*: The model apicomplexan. *International Journal for Parasitology* 34 (3): 423–432. <https://doi.org/10.1016/j.ijpara.2003.12.009>.
- Kleczkowski, L.A., D. Decker, and M. Wilczynska. 2011. UDP-sugar pyrophosphorylase: A new old mechanism for sugar activation. *Plant Physiology* 156 (1): 3–10. <https://doi.org/10.1104/pp.111.174706>.
- Krishnan, A., and D. Soldati-Favre. 2021. Amino acid metabolism in apicomplexan parasites. *Metabolites* 11 (2): 61. <https://doi.org/10.3390/metabo11020061>.
- Lourido, S. 2019. *Toxoplasma gondii*. *Trends in Parasitology* 35 (11): 944–945. <https://doi.org/10.1016/j.pt.2019.07.001>.
- Lyons, R.E., R. McLeod, and C.W. Roberts. 2002. *Toxoplasma gondii* tachyzoite-bradyzoite interconversion. *Trends in Parasitology* 18 (5): 198–201. [https://doi.org/10.1016/S1471-4922\(02\)02248-1](https://doi.org/10.1016/S1471-4922(02)02248-1).
- Lyu, C., X. Yang, J. Yang, L. Hou, Y. Zhou, J. Zhao, et al. 2021. Role of amylopectin synthesis in *Toxoplasma gondii* and its implication in vaccine development against toxoplasmosis. *Open Biology* 11 (6): 200384. <https://doi.org/10.1098/rsob.200384>.
- Mahlow, S., S. Orzechowski, and J. Fettke. 2016. Starch phosphorylation: Insights and perspectives. *Cellular and Molecular Life Sciences* 73 (14): 2753–2764. <https://doi.org/10.1007/s00018-016-2248-4>.
- Pittman, K.J., M.T. Aliota, and L.J. Knoll. 2014. Dual transcriptional profiling of mice and *Toxoplasma gondii* during acute and chronic infection. *BMC Genomics* 15 (1): 806. <https://doi.org/10.1186/1471-2164-15-806>.
- Ryley, J.F., M. Bentley, D.J. Manners, and J.R. Stark. 1969. Amylopectin, the storage polysaccharide of the *Coccidia* *Eimeria brunetti* and *E. tenella*. *The Journal of Parasitology* 55 (4): 839–45. <https://doi.org/10.2307/3277227>.
- Shen, B., and L.D. Sibley. 2014. *Toxoplasma* aldolase is required for metabolism but dispensable for host-cell invasion. *Proceedings of the National Academy of Sciences* 111 (9): 3567–3572. <https://doi.org/10.1073/pnas.1315156111>.
- Shen, B., K.M. Brown, T.D. Lee, and L.D. Sibley. 2014. Efficient gene disruption in diverse strains of *Toxoplasma gondii* using CRISPR/CAS9. *mBio* 5 (3): e01114-14. <https://doi.org/10.1128/mBio.01114-14>.
- Shen, B., K. Brown, S. Long, and L.D. Sibley. 2017. Development of CRISPR/Cas9 for efficient genome editing in *Toxoplasma gondii*. *Methods in Molecular Biology* 1498: 79–103. https://doi.org/10.1007/978-1-4939-6472-7_6.
- Sugi, T., V. Tu, Y. Ma, T. Tomita, and L.M. Weiss. 2017. *Toxoplasma gondii* requires glycogen phosphorylase for balancing amylopectin storage and for efficient production of brain cysts. *mBio* 8 (4): e01289-17. <https://doi.org/10.1128/mBio.01289-17>.
- Tomavo, S. 2015. Too much sugar puts a parasite in jeopardy. *Cell Host & Microbe* 18 (6): 641–643. <https://doi.org/10.1016/j.chom.2015.11.013>.
- Tu, V., R. Yakubu, and L.M. Weiss. 2018. Observations on bradyzoite biology. *Microbes and Infection* 20 (9–10): 466–476. <https://doi.org/10.1016/j.micinf.2017.12.003>.
- Uboldi Alessandro, D., M. McCoy James, M. Blume, M. Gerlic, J.P. Ferguson David, F. Dagley Laura, et al. 2015. Regulation of starch stores by a Ca²⁺-dependent protein kinase is essential for viable cyst development in *Toxoplasma gondii*. *Cell Host & Microbe* 18 (6): 670–81. <https://doi.org/10.1016/j.chom.2015.11.004>. <https://www.sciencedirect.com/science/article/pii/S1931312815004588>.
- Wang, Q.-Q., K. He, M.-T. Aleem, and S. Long. 2023. Prenyl transferases regulate secretory protein sorting and parasite morphology in *Toxoplasma gondii*. *International Journal of Molecular Sciences* 24 (8): 7172. <https://doi.org/10.3390/ijms24087172>. <https://www.mdpi.com/1422-0067/24/8/7172>.
- Xia, N., J. Yang, S. Ye, L. Zhang, Y. Zhou, J. Zhao, et al. 2018. Functional analysis of *Toxoplasma* lactate dehydrogenases suggests critical roles of lactate fermentation for parasite growth in vivo. *Cellular Microbiology* 20 (1): e12794. <https://doi.org/10.1111/cmi.12794>.
- Xia, N., S. Ye, X. Liang, P. Chen, Y. Zhou, R. Fang, et al. 2019. Pyruvate homeostasis as a determinant of parasite growth and metabolic plasticity in *Toxoplasma gondii*. *mBio* 10 (3): e00898-19. <https://doi.org/10.1128/mBio.00898-19>.

- Xu, Q., Y.-Y. Duan, M. Pan, Q.-W. Jin, J.-P. Tao, and S.-Y. Huang. 2023. In vitro evaluation reveals effect and mechanism of artemether against *Toxoplasma gondii*. *Metabolites* 13 (4): 476. <https://doi.org/10.3390/metabo13040476>.
- Yang, J., L. Zhang, H. Diao, N. Xia, Y. Zhou, J. Zhao, et al. 2017. ANK1 and DnaK-TPR, two tetratricopeptide repeat-containing proteins primarily expressed in *Toxoplasma bradyzoites*, do not contribute to bradyzoite differentiation. *Frontiers in Microbiology* 8: 2210. <https://doi.org/10.3389/fmicb.2017.02210>.
- Yang, J., C. Yang, J. Qian, F. Li, J. Zhao, and R. Fang. 2020. *Toxoplasma gondii* α -amylase deletion mutant is a promising vaccine against acute and chronic toxoplasmosis. *Microbial Biotechnology* 13 (6): 2057–2069. <https://doi.org/10.1111/1751-7915.13668>.
- Yang, J., Z. He, C. Chen, J. Zhao, and R. Fang. 2022. Starch branching enzyme 1 is important for amylopectin synthesis and cyst reactivation in *Toxoplasma gondii*. *Microbiology Spectrum* 10 (3): e0189121. <https://doi.org/10.1128/spectrum.01891-21>.
- Ye, S., N. Xia, P. Zhao, J. Yang, Y. Zhou, B. Shen, et al. 2019. Micronemal protein 13 contributes to the optimal growth of *Toxoplasma gondii* under stress conditions. *Parasitology Research* 118 (3): 935–944. <https://doi.org/10.1007/s00436-018-06197-3>.

Publisher's Note

Springer Nature remains neutral with regard to jurisdictional claims in published maps and institutional affiliations.

Ready to submit your research? Choose BMC and benefit from:

- fast, convenient online submission
- thorough peer review by experienced researchers in your field
- rapid publication on acceptance
- support for research data, including large and complex data types
- gold Open Access which fosters wider collaboration and increased citations
- maximum visibility for your research: over 100M website views per year

At BMC, research is always in progress.

Learn more biomedcentral.com/submissions

